

ANALYSIS OF RESTRAINED COMPOSITE PERFORATED BEAMS DURING FIRE USING A HYBRID SIMULATION APPROACH

Mustesin Ali Khan¹, Katherine A Cashell², Asif S. Usmani³

Abstract

This paper is concerned with the behaviour of restrained perforated beams acting compositely with a profiled slab during a fire. These members are increasingly popular in the construction of long-span floor systems as they provide a structurally and materially efficient design solution and provide space for placement of building services. However, their response during a fire has received little attention from the research community until recently. In the current work, a hybrid simulation-type numerical approach is adopted using a combination of the OpenSEES, ABAQUS and OpenFresco software. The accuracy of the model is validated using available fire test data whereby the temperatures measured during the experiments are directly applied in the numerical model at various locations. The effect of axial and rotational restraint due to the connections between the beams and columns is also investigated following validation of the model. Furthermore, the hybrid simulation approach is employed to study a number of salient parameters, including load ratios, material grade and the location of the openings. The variation in axial force during the fire is also examined. Various failure modes are observed during the analysis including flexural and shear failure, failure of the web-post, concrete crushing and also a Vierendeel mechanism. The fire resistance of the analysed beams is compared with the values obtained from the most common design codes. Due to the consideration of restraint forces, which are not included in the design codes, the resistances predicted by the finite element simulations are more favourable. It is found that the location of the openings along the span and also the boundary conditions have a considerable effect on the time-displacement behaviour, axial reactions, web-post buckling behaviour as well as the fire performance of the perforated beam.

¹ PhD Candidate. Department of Civil and Environmental Engineering, Brunel University London, London, UK. e-mail: mustesin.khan@brunel.ac.uk

² Senior Lecturer. Department of Civil and Environmental Engineering, Brunel University London, London, UK. e-mail: katherine.cashell@brunel.ac.uk

³ Professor. Department of Building Services Engineering, The Hong Kong Polytechnic University, Hong Kong. e-mail: asif.usmani@polyu.edu.hk

1 INTRODUCTION

2 In modern construction of steel framed buildings, there is an increasing tendency towards the
3 specification of long-span floor systems which enable larger open plan spaces to be achieved.
4 Perforated or cellular beams composite with a reinforced concrete floor slab are a popular
5 choice for such floor systems. Perforated beams can be made either by cutting and welding
6 hot-rolled steel sections to provide the desired shape or by fabricating the section from steel
7 plates. The openings may be designed in any shape but the most popular ones are circular
8 (giving a cellular beam), rectangular, elongated and sinusoidal openings. These are separated
9 by solid web-posts and the web-post size varies according to the dimensions of the openings.
10 Generally, perforated beams are preferred in multi-storey buildings to regular I sections as they
11 allow for longer spans to be achieved which, in turn, leads to more flexible column-free space
12 and shorter erection times. In addition, they can reduce the overall height of the building owing
13 to the integration of services within the structural frame. It has been shown that using these
14 types of beam can be very economical and reduce the total weight of steel work significantly
15 (Nadjai et al. 2017).

16 The behaviour of structures in fire has been the subject of intensive research in recent decades
17 (British Steel Plc 1999; Dwaikat and Kodur 2011; Li and Guo 2008; Liu et al. 2002) and is
18 particularly topical at the current time following the building fire at Grenfell Tower in London
19 in 2017. Due to the many complexities involved, most research focusses on the response of
20 isolated structural elements, without necessarily including the whole structure in the analysis,
21 usually idealising the effect of surrounding elements. There have been considerably more
22 analytical studies and fire tests on simply supported cellular beams (Ellobody and Young 2015;
23 Nadjai et al. 2007, 2016; Wong et al. 2009), compared with those that are axially and/or
24 rotationally restrained. This is despite the fact that the majority of composite perforated beams
25 in practice experience some degree of both axial and rotational restraint, and their behaviour is
26 very dependent on the type and magnitude of the restraint provided by the surrounding
27 structure.

28 Large-scale structural fire tests are rare because they are very costly and require specialized
29 experimental facilities. Most of the experimental research into the behaviour of structures in
30 fire has been carried out on isolated structural components, exposed to standard fire curves, in
31 order to compare the fire performance under similar testing conditions. However, they do not
32 represent real fires and building elements such as beams, floors, walls and columns are usually
33 examined without taking into account the effect of the surrounding structural components. This
34 is particularly important when a statically indeterminate structural assembly is subjected to fire
35 because it experiences indirect loadings due to the restrained thermal deformations, i.e., a
36 compressive force is induced in the member when it begins to expand but is restrained from
37 doing so. Upon failure of the fire exposed member in an indeterminate structure, the load is

1 transferred to other members; this load redistribution may save the structure from collapse. In
2 light of the benefits and challenges of structural fire testing, hybrid simulation has emerged as
3 a promising technique in that it combines testing of isolated components with simultaneous
4 coupled simulation of the global response.

5 In this context, the current paper is focused on the fire behaviour of restrained perforated steel
6 beams which are acting compositely with a profiled slab. One of the largest studies into
7 restrained perforated beams under fire conditions was done by researchers at the University of
8 Ulster and the Czech Technical University (Wald et al. 2011; Najjai et al. 2011, 2017). This
9 work included two full-scale fire tests. These were very informative tests which monitored
10 many of the variables which affect the response. However, end displacements at the ends of
11 the beams were not measured during the tests although these are important parameters in terms
12 of the overall building behaviour as well as the ultimate fire resistance of these members. Najafi
13 and Wang (Najafi and Wang 2017a; b) developed both a numerical and analytical model to
14 investigate the behaviour of restrained cellular beams at elevated temperature. In this study, the
15 level of axial restraint provided was assessed and considered, however the influence of a
16 composite slab was not included nor was the effects of rotational restraint.

17 A simplified analysis of a frame comprising cellular beams exposed to fire was performed by
18 Abu (Abu et al. 2009). In this study, the effect of the openings was incorporated by considering
19 an equivalent web thickness, resulting in a solid beam. Although this was a useful investigation
20 in many ways, this approach cannot predict the failure modes associated specifically with
21 perforated beams such as web-post buckling and the Vierendeel mechanism. In general, there
22 is a lack of data on the behaviour of restrained composite perforated beams exposed to fire.
23 Accordingly, the work presented in the current paper aims to bridge this gap and study the
24 behaviour using a hybrid simulation-type numerical approach. This modelling method is
25 employed because it is capable of analysing the whole structure in an accurate yet
26 computationally efficient manner. The structure is divided into two sub-sections, or assemblies,
27 and the area which is expected to behave nonlinearly and undergo large deformations is
28 modelled in fine numerical detail in one assembly whilst the rest of the structure which behaves
29 elastically is modelled in another assembly at a much lower computational cost. A middleware
30 or interaction software such as UI-SIMCOR or OpenFresco (Kwon et al. 2007; Takahashi and
31 Fenves 2006) is used at the interface to transfer data from one assembly to the other and vice
32 versa. To date, hybrid simulation is most commonly used in earthquake engineering although
33 it is very useful for studying the effect of other extreme events, such as a fire, as will be
34 presented in the current paper.

35 **VIRTUAL HYBRID SIMULATION**

1 In this section, hybrid simulation and virtual hybrid simulation are described, with a particular
2 emphasis on their use for analysing structural response in fire. This is followed by a description
3 of the virtual hybrid simulation approach that has been developed in the current work.

4 ***Background to Hybrid Simulation and Virtual Hybrid Simulation***

5 Hybrid simulation (HS) is most commonly employed by earthquake engineers to study the
6 seismic behaviour of structures. In this computational method, the structure is divided into two
7 assemblies or substructures. The assembly which is expected to experience large deformations
8 or whose seismic performance needs to be evaluated in fine detail is tested physically in the
9 laboratory and is known as the physical substructure (PS). The rest of the structure is modelled
10 using a standard FE software in the other assembly which is referred to as the numerical
11 substructure (NS). Both assemblies interact with each other at each time step of the response
12 using a communication software e.g., OpenFresco. In summary, performing a hybrid
13 simulation involves the following steps:

- 14 1. The NS is started and calculates the displacements and rotations at the interface for the
15 first time-step.
- 16 2. These displacements and rotations are applied to the PS in the laboratory through the
17 actuators, which are directly connected to the FE model (NS).
- 18 3. The reaction forces and moments as a result of the applied displacement and rotations
19 in the physical test are recorded at the interface of the PS and then fed back to the NS
20 to perform the next integration step and determine the new set of displacements and
21 rotations. These steps are repeated until the end of the test.

22 Using this technique, it is possible to apply real boundary conditions owing to the surrounding
23 structure to the PS in the laboratory and obtain an accurate depiction of the whole system
24 behaviour. Although this approach is relatively common in seismic engineering, there are few
25 examples in the literature of hybrid simulation being applied to analyse structures exposed to
26 fire. Mostafaei (Mostafaei 2013) conducted a hybrid analysis of a reinforced concrete frame,
27 including a fire test of the first floor central column. The rest of the structure was modelled in
28 the non-linear finite element software SAFIR (Franssen and Gernay 2017). Utilising the
29 symmetry of the structure, the substructures interacted with each other through manual control
30 of the axial force at the column ends. The interaction between the physical and numerical
31 substructures was not automatic but was user-controlled, meaning that the user paused the
32 physical test every five minutes to log the numerical data and then the simulation was re-started.
33 The accuracy of this approach was compromised due to the manual nature of the test.

34 More recently, Whyte et al. (2016) performed the first fully-automated hybrid simulation in
35 fire. The experiment was carried out in the elastic range on a scaled specimen which was
36 exposed to temperatures up to 200°C. While it was the first fully-automated hybrid fire
37 simulation, the methodology requires further validation for large-scale specimens subjected to

1 realistic fires. Another hybrid fire testing method was proposed by Sauca et al. (2018), in which
2 a hybrid simulation is performed entirely in a numerical environment. This method is fully
3 automated and displacement-controlled. In these numerical simulations, the integration model
4 is defined as a stiffness matrix and the substructure model is simulated in the FE software,
5 SAFIR.

6 In further developments, Wang et al. (2018) conducted a hybrid fire simulation by testing a
7 central ground-floor column in the laboratory whilst simultaneously modelling the surrounding
8 structure in ABAQUS. To transfer the data between two substructures, a network interface
9 program called NICON was employed (Zhan and Kwon 2015). Similar to other arrangements,
10 this test also utilised the symmetry of the structure and the substructures interacted with each
11 other through the control of axial forces and displacements at the column interface.

12 The stability of hybrid simulation in a numerical environment is rarely compromised during
13 the data exchange between the two substructures. However, the accuracy of the model can be
14 affected by the size of the time step and also the mesh size and structure. The time step used in
15 both assemblies should be sufficiently small to avoid instability without compromising the
16 efficiency of the model. A large time step may also lead to noise in the solution. The mesh
17 employed in the slave assembly is also important. An irregular mesh may result in development
18 of stress concentrations and lead to unrealistic results. Moreover, the mesh size should be small
19 enough to capture all important behavioural features of the model with reasonable accuracy
20 while minimising the computational effort.

21 In a real hybrid fire test with a physical specimen, many factors can introduce instabilities
22 during the test. Since the fire exposure is time dependent, the time interval required to perform
23 the calculations for the NS and to apply the interfacial actions and displacements to the PS may
24 become a source of error, because while the interface data is calculated, the PS continues to be
25 exposed to fire loading. Therefore the calculated interface data may not be in agreement with
26 altered state of the PS and the equilibrium and compatibility requirements at the interface may
27 not be satisfied. The time interval required to apply the target values on the PS therefore need
28 to be carefully estimated and implemented to avoid instability in real HFT. The other most
29 common factor affecting the results of hybrid simulation are the experimental errors associated
30 with the data transfer system. A poorly tuned transfer system may induce errors by not being
31 able to impose the calculated response quantities accurately, which is not an issue for VHFT.

32 Hybrid simulation in a real fire testing scenario is very complex, particularly if it is necessary
33 to apply manual control to more than one interface. There are up to six unknowns (i.e. degrees
34 of freedom in the NS and forces and moments in the PS) requiring control and communication
35 at each interface. Manual control of these quantities increases the complexity of the tests and
36 can introduce error into the process. So, before conducting a hybrid simulation in fire it is
37 necessary to establish a hybrid simulation framework in a numerical environment. This means

1 replacing the physical testing element of the hybrid simulation with another numerical model
2 which uses high resolution elements such as 3D shell and brick elements to create a so-called
3 virtual hybrid simulation approach. The successful implementation of a virtual hybrid
4 simulation framework eliminates the requirement for manual involvement between the two
5 assemblies and this system can then be employed with a physical substructure in place of the
6 detailed FE model in future work. In this approach, a multiple number of responses can be
7 controlled and communicated at the interface between the two assemblies.

8 *Development of the Virtual Hybrid Simulation Method*

9 The current paper is concerned with the development of a virtual hybrid simulation framework
10 which has been developed using both the ABAQUS (ABAQUS 2010) and OpenSEES
11 (McKenna et al. 2009) finite element (FE) analysis software's. There are many different FE
12 packages available for commercial and research purposes which can provide an efficient and
13 inexpensive method for analysing the behaviour of structures exposed to extreme events, such
14 as fire. However, most commercial software does not allow developers to implement their own
15 source code and therefore open-source software such as OpenSEES is advantageous for
16 developing novel simulation techniques such as virtual hybrid simulation.

17 In the current work, the detailed numerical modelling (replicating the PS in hybrid simulation)
18 is simulated in the ABAQUS software (ABAQUS 2010) in what is termed the slave assembly.
19 ABAQUS is employed as it provides specific capabilities for the high-fidelity material
20 modelling, including capturing nonlinear local failures such as local buckling of the steel
21 section and crushing or cracking of the concrete. The other assembly, referred to as the master
22 assembly, represents the surrounding structure and is modelled in the OpenSEES software
23 using simpler beam-column elements. Traditionally, OpenSEES has been selected as the
24 preferred software for hybrid simulations in earthquake engineering. Building on this
25 experience, OpenSEES has been developed for fire engineering, such that it can accurately
26 model the response of framed structures subjected to realistic fire scenarios (such as travelling
27 fires, for example), which is currently not possible in other FE softwares. Moreover,
28 OpenSEES capability in earthquake response simulation also provides the capability of multi-
29 hazard simulations in future advancements. Therefore, OpenSEES is selected in the current
30 work because it an open-source software and is capable of providing an accurate depiction of
31 the global or system-level nonlinear structural response in extreme conditions such as a fire.

32 *OpenSEES*

33 OpenSEES is an open-source finite element analysis software which was originally developed
34 for earthquake engineering applications at the University of California, Berkeley (McKenna et
35 al. 2009; McKenna 1997). Owing to its open-source framework, OpenSEES is a collaborative
36 programme which allows developers to add components to the original source code depending
37 on their particular needs, and then disseminate these developments to other potential users. It

1 is constantly being developed by researchers for different types of application (Kolozvari et al.
2 2018; Zhu et al. 2018), including structural fire engineering (Jiang et al. 2015; Jiang and
3 Usmani 2018a; b). OpenSEES is an object-oriented software implemented in the C++
4 programming language, using the 'Tcl' scripting language.

5 In the virtual hybrid simulation approach, both the master and slave assemblies interact at the
6 interface nodes at each integration step. This is facilitated using the middleware OpenFresco
7 which transfers the boundary conditions and reaction forces between the master and slave
8 assemblies. A super element and an adapter element are defined in the slave and master
9 assemblies, respectively, to couple the two models (if using the same software for PS and NS)
10 or two software packages. The displacements and rotations that are calculated in the master
11 programme (i.e. representing the whole structure) are implemented as boundary conditions in
12 the slave assembly when investigating the detailed response of the perforated beam under fire
13 conditions. Subsequently, the slave programme estimates the corresponding reaction forces and
14 returns them to the master. This approach presents an alternative to modelling the whole
15 structure in 3D using high resolution elements which is both complex and computationally
16 expensive.

17 *OpenFresco*

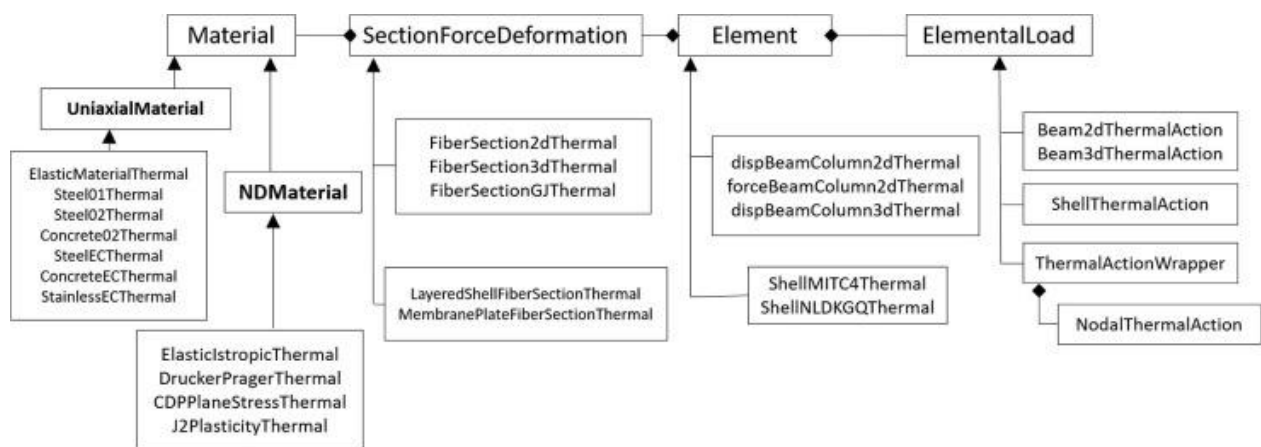
18 There are a number of different approaches for enabling the two assemblies to communicate
19 with each other. The most traditional method is to use a file exchange system, which has been
20 implemented in a number studies (Kolozvari et al. 2018; Kwon et al. 2007). In this system, the
21 trial displacements and rotations are firstly estimated by the master FE code at the interface
22 and saved in the form of data files. Then, the saved quantities are applied as boundary
23 conditions in the slave assembly and the reaction forces at the interface node are estimated.
24 These responses are also stored in a similar way in data files. Finally, the stored reaction forces
25 are applied at the interface node in the master assembly to determine the new displacements
26 and rotations for the next time step. The above steps are repeated for each integration time step
27 until the end of the analysis. Although the file exchange system provides an effective means
28 for transferring data between the two assemblies, the main disadvantage is that the two FE
29 models cannot run concurrently and therefore it is not very computationally efficient.

30 In the current study, the data is transferred between the two codes using a middleware software
31 called OpenFresco. Using this method for data communication between the two programmes
32 enables both FE codes to run simultaneously, without restarting the analysis at every time step.
33 This reduces the complexity and enhances the computational efficiency of the process,
34 compared with the file exchange system. Accordingly, OpenFresco facilitates the storage,
35 transformation and transfer of data between the master and slave assemblies.

36 *Thermomechanical Analysis in OpenSEES*

1 Elevated temperature finite element analysis is conducted in OpenSEES in two stages. First, a
 2 heat transfer analysis is conducted in which a fire is applied to the structure in the form of a
 3 time-temperature relationship and then the resulting temperatures at various points in the
 4 structure are determined. Secondly, the temperature history data from the heat transfer analysis
 5 is used in the thermo-mechanical stress analysis to assess how the structure responds to the
 6 applied loads during a fire. Both the thermal strains and the temperature-dependent material
 7 properties are considered in the thermo-mechanical analysis. In the current study, there is no
 8 requirement to conduct a heat transfer analysis as the temperatures at various points in the
 9 structure are taken directly from the test data and input into the thermo-mechanical model. The
 10 class hierarchy in the implementation of the thermo-mechanical element is illustrated in Fig. 1,
 11 where ‘Material’, ‘SectionForce Deformation’, ‘Element’ and ‘ElementalLoad’ are all abstract
 12 (or base) classes and the others such as ‘UniaxialMaterial’ and ‘NDMaterial’ are the derived
 13 classes. The beam-column element used in this study to model the structural frame is
 14 formulated based on interpolation of the displacement or force. A range of uniaxial material
 15 classes are available in the OpenSEES and the mechanical and thermal properties employed in
 16 the current study are taken from the Eurocodes (EN-1994-1-2 2005; EN 1992-1-2 2004; EN
 17 1993-1-2 2005).

18



19

20

Fig. 1. Classes developed in OpenSEES for thermo-mechanical analysis

21 IMPLEMENTATION OF THE VIRTUAL HYBRID SIMULATION APPROACH

22 The virtual hybrid simulation approach is validated using the fire test which was conducted on
 23 an administrative building in Mokrsko by the Czech Technical University (Wald et al. 2011).
 24 The experimental structure represented one floor of an administrative building which was 12
 25 × 18 m in floor area, with a height of 4 m. This included a composite cellular beam which was
 26 subjected to fire, known as the AS4 composite cellular beam. The schematic for this test is
 27 shown in Fig. 2 (a). Beam AS4 was made using an IPE270 I-beam in grade S235 steel which
 28 was cut to create sinusoidal openings giving an overall depth of 395 mm. The concrete slab
 29 had an overall depth of 120 mm, comprising a flat portion and ribs which were 60 mm each in

1 depth, as shown in Fig. 2 (b). The compressive strength of the concrete was 32.5 MPa with a
2 mass density of 2400 kg/m^3 . The slab reinforcement was located at the mid-depth of the flat
3 portion of the slab, was 5 mm in diameter, and was positioned at 100 mm centres in both
4 directions. It had a yield strength of 500 N/mm^2 and the cover distance to the edge of the
5 concrete was 20 mm. IPE 400 sections were used for the edge beams, which were also in grade
6 S235 steel, whilst the columns were made using HEB 180 sections. The adjacent beams were
7 made using a WTB 500 section made from grade S320 steel. The test was performed in two
8 stages. Firstly, a mechanical load of 5.6 kN/m^2 was applied uniformly to the floor, representing
9 a load ratio of 0.26. Then, the load was maintained at a constant level whilst the elevated
10 temperature was applied as shown in Fig. 3 (Wald et al. 2011).

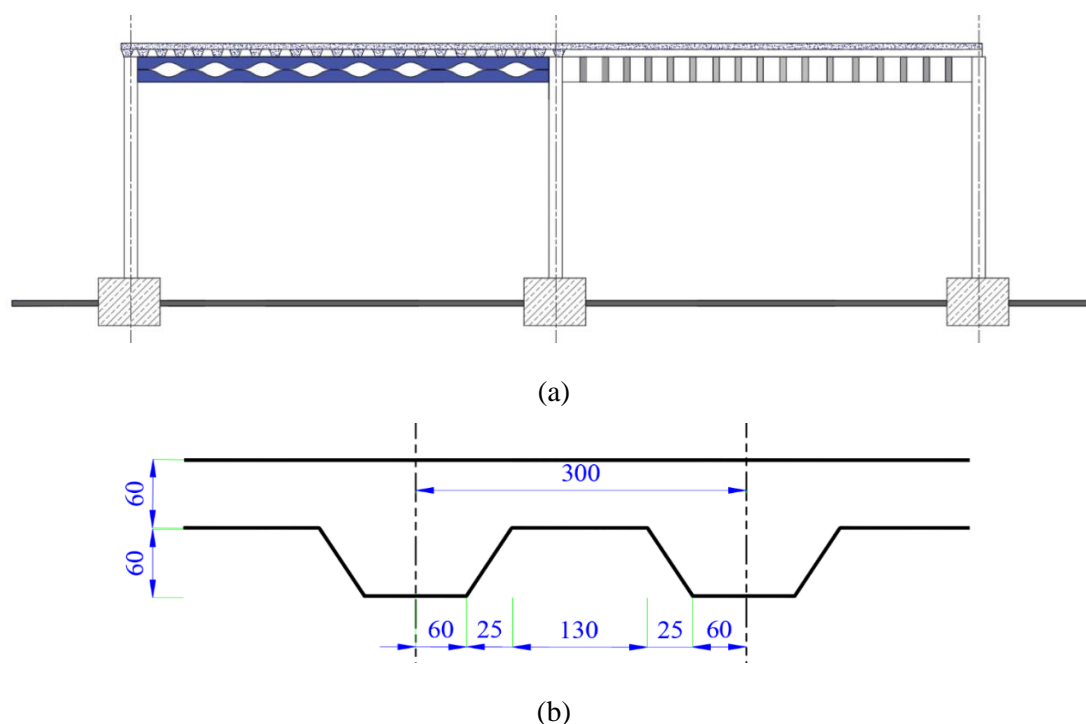


Fig. 2. (a) Schematic for Mokrosko fire test (b) Profiled deck slab (all dimensions are in mm)

16 In order to represent this test arrangement in the virtual hybrid simulation, the fire exposed
17 perforated beam is modelled as slave structure in ABAQUS using a high resolution mesh of
18 3D shell elements for perforated steel beam and 3D solid elements for the concrete slab whilst
19 beam-column elements are utilised for the rest of the structure in the master assembly in
20 OpenSEES. The schematic for both the master and slave assemblies is shown in Fig. 4. This
21 approach investigates the behaviour of the fire-exposed perforated beam while including the
22 effect of remaining structure without modelling the whole system in 3D. So, it provides a
23 computationally efficient methodology for analysing the whole structural system in fire. It is
24 noteworthy that in the Mokrosko fire test, the slab lost its resistance in compression and no
25 two-way tensile membrane action was reported to have developed. Although it is intuitively
26 advantageous to model the whole structure in as much detail as possible, to trace the real

1 behaviour of structures in fire, it can add unnecessary complexity. In this case, modelling the
2 entire slab up to its perimeter accounting for two-way action is not required as no two-way
3 action developed, and therefore one-way composite beam action is assumed in the model for
4 the sake of simplicity.

5 The steel beam is represented using S4R shell elements which are available in the ABAQUS
6 library, and each element is 25×25 mm in size, based on a mesh sensitivity study. The concrete
7 slab is modelled using C3D8R solid elements while the reinforcement is modelled using T3D2
8 truss elements. The steel decking is not included in the model as it is not expected to have a
9 significant influence on the fire behaviour. The connection between the perforated beam and
10 the deck slab is represented using the tie constraint in ABAQUS. In terms of material
11 modelling, it is assumed that the steel behaves in an elastic-plastic manner whilst the concrete
12 damaged plasticity model is employed to represent the concrete. The stress-strain relationship
13 for both concrete and steel at elevated temperature is adopted from the Eurocode (EN 1992-1-
14 2 2004; EN 1993-1-2 2005). For the thermal properties, constant values of $0.000014 / ^\circ\text{C}$ and
15 $0.000009 / ^\circ\text{C}$ are used for the coefficient of thermal expansion of steel and concrete,
16 respectively. The remainder of the frame comprising the adjacent beam (WTB 500) which is
17 modelled as section IPE 400 (section used for edge beams) and columns are modelled as section
18 HEB 180 using 3D beam-column elements in the master assembly in OpenSEES.

19 At the interface between the master and slave assemblies, OpenFresco requires that an adapter
20 element and a super element are defined in the slave and master assemblies, respectively. For
21 the 2-node adapter element in the slave assembly, the nodes at the left and right of the
22 perforated beam are constrained as shown in Fig. 4. This element effectively applies the
23 boundary conditions at the interface degrees of freedom of the perforated beam. A very high
24 stiffness value of 1×10^{12} N/mm is employed for the diagonal element of the stiffness matrix
25 to ensure that the boundary conditions are accurately represented (Schellenberg et al. 2008).
26 The kinematic compatibility of the approach has been described in more detail elsewhere (Khan
27 et al. 2018). Similarly, a 2-node super element is defined at the interface nodes in the master
28 assembly. The initial stiffness matrix for the super element is determined by applying a unit
29 displacement to the perforated beam model in ABAQUS and measuring the resulting force. As
30 in the test, the analysis is performed in two stages, with a mechanical load applied first,
31 followed by the fire loading.

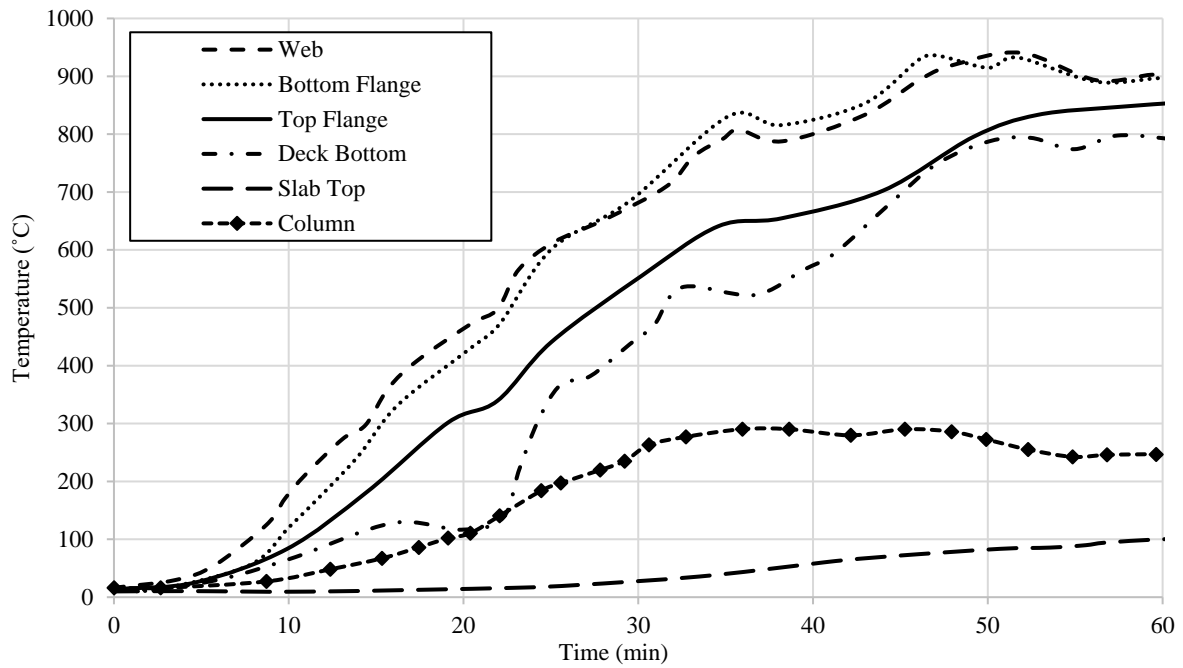


Fig. 3. Temperature profile at the various locations (Wald et al. 2011)

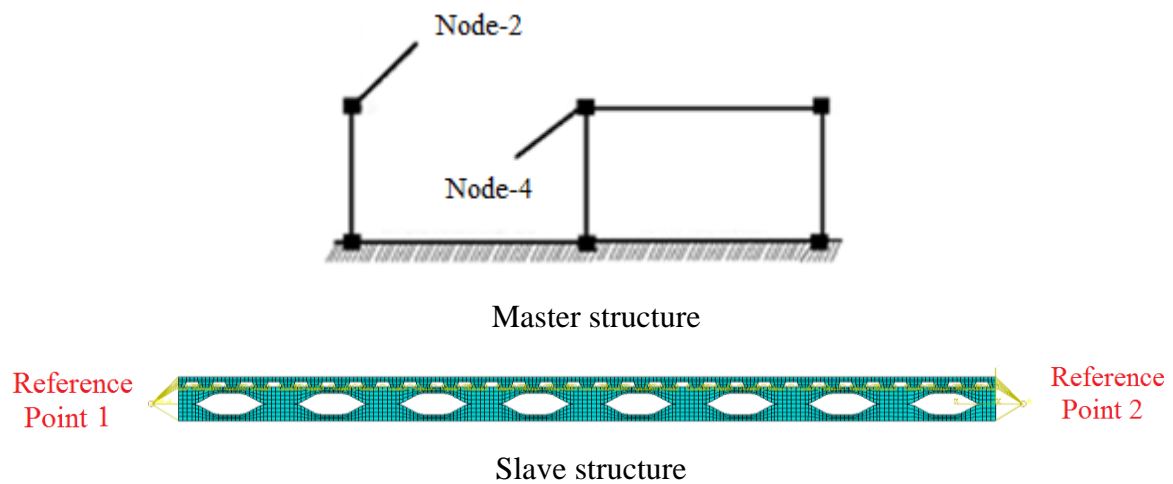


Fig. 4. Sub-structuring for hybrid simulation

During the simulation, firstly the displacements at the interface nodes are determined in the master assembly. Then, these displacements are communicated and applied at the interface nodes in the slave assembly. The reaction forces are calculated in the slave assembly and applied at the interface nodes of the master assembly for the determination of the new displacement. The communication between the two codes and the development of the model is presented in Fig. 5 and outlined as:

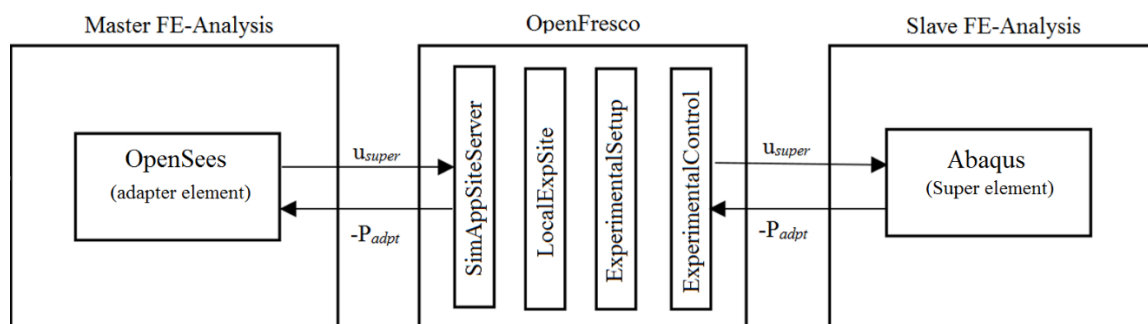
Step 1: The master programme analysis commences and generates a displacement vector for the global trial displacements (u_{super}) at the interface degrees of freedom. u_{super} is then sent to the super element by the master assembly.

1 Step 2. The TCP/IP socket (where TCP/IP means a Transmission Control Protocol/Internet
2 Protocol which is the basic communication language or protocol for the internet) is used to
3 send u_{super} to OpenFresco and the simulation server process begins.

4 Step 3. Other objects i.e., the 'LocalExpSite' and 'ExperimentalSetup' classes (see Fig. 5)
5 are used to store and transform u_{super} . Data transformation is not required in this study because
6 no physical specimen (i.e. laboratory test specimen) is used. So, the 'NoTransformation' object
7 as 'ExpSetup' is utilised.

8 Step 4. The u_{super} element is then transferred to the 'ExperimentalControl' object which feeds
9 the trial displacement vector to the adapter element in the slave assembly, using a TCP/IP
10 socket. A resultant displacement vector is formed by the adapter element by combining u_{super}
11 with its own elemental displacements. Subsequently, the resultant element force vector (P_{adpt})
12 is also updated by the adapter element.

13 Step 5. Upon convergence in the slave programme, the negative resultant force vector ($-P_{adpt}$)
14 is communicated to the 'ExperimentalControl' object through the TCP/IP socket.
15 'LocalExpSite' and 'ExperimentalSetup' objects are again utilised for the storage and
16 transformation of the force vector (see Fig. 5).



17
18 Fig. 5. Sequence of operations and data exchange

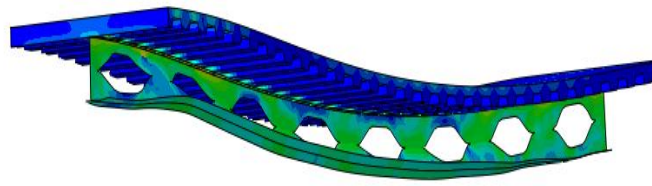
19 Step 6. The force vector is transferred to the super element in the master programme by
20 'SimAppSiteServer' object through the TCP/IP socket.

21 Step 7. $-P_{adpt}$ is saved as element forces by the super element and returned to the master
22 integration method for the next step. The new trial displacement vector is calculated by the
23 master programme and Step 1 to Step 7 are repeated until the analysis is complete.

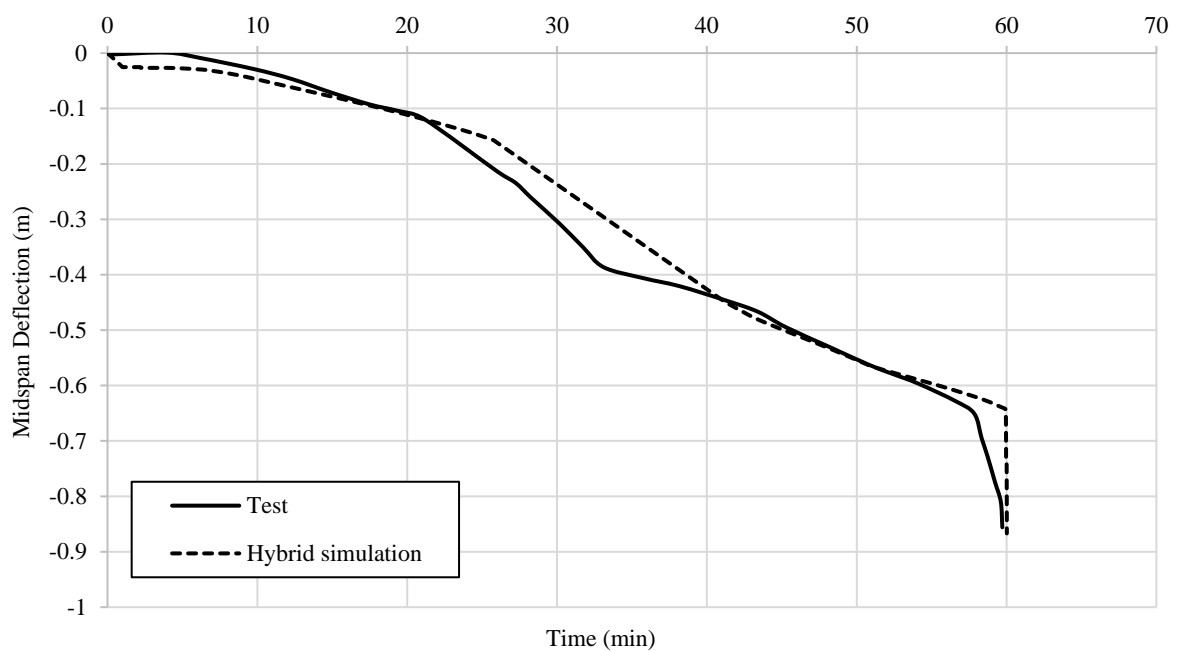
24 VALIDATION AND PARAMETRIC STUDY

25 In this section, the virtual hybrid simulation approach is applied to the experiment conducted
26 at Mokrsko and described previously (Wald et al. 2011). Fig. 6 presents the deformed shape
27 predicted by the finite element simulation. The images show that during the fire, the bottom
28 flange of the beam displaced laterally which caused the steel web to bend. Meanwhile, the top
29 flange was restrained by the composite slab. The midspan vertical deflection of the restrained

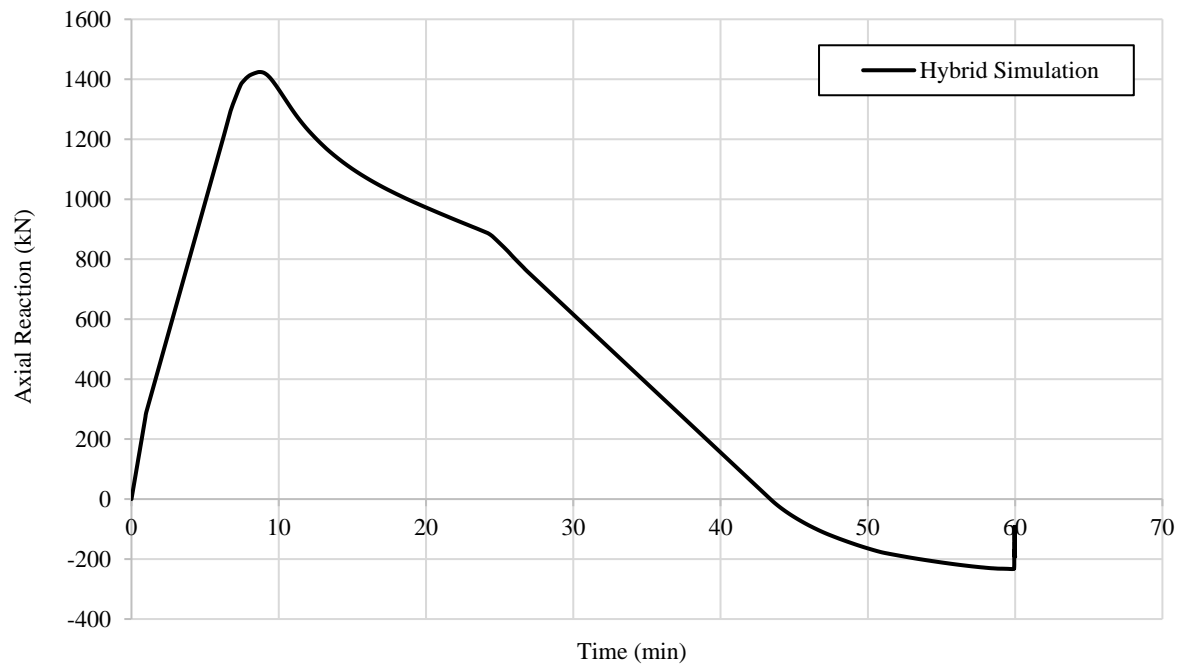
1 composite perforated beam (AS4) as predicted by the hybrid simulation is plotted against time
2 and compared with the test results in Fig. 7 and it is shown that a good agreement is obtained.
3 Fig. 8 presents the variation in axial reaction during the fire, as predicted by the virtual hybrid
4 simulation (measurements from the test are not available). Initially, it is shown that the beam
5 experiences axial compression (indicated by a positive value in Fig. 8) due to restrained thermal
6 expansion which increases until the onset of local buckling in the steel section. Subsequently,
7 the compressive forces reduce due to the significant changes in material stiffness at high
8 temperature, and the axial forces change from compression to tension as the full cross-section
9 goes into tension and behaves like a tensile catenary.



10
11 Fig. 6. Deformed shape of the perforated test beam



13
14 Fig. 7. Vertical deflection of the AS4 beam during the fire



1

2

Fig. 8. Axial reaction at the beam support, with time, for beam AS4

3

Following this validation, the model is employed to conduct an extensive parametric study to analyse the response of restrained composite perforated beams in fire. The effect of load ratio, steel strength and opening position on the behaviour is studied. The various parameters considered in the study are summarised in Table 1, including three different load levels (namely LL1=3.1 kN/m², LL2=4.3 kN/m² and LL3=5.6 kN/m², respectively) and three grades of steel (with yield strengths of 275, 450 and 550 N/mm², respectively). Four opening layouts are considered in the parametric study which are presented in Fig. 9, and described as follows:

10

Layout 1: Openings in the centre of the beam (bending zone);

11

Layout 2: Openings at 250 mm from the one end (one shear zone);

12

Layout 3: Openings at 250 mm from both the ends (both shear zones); and

13

Layout 4: Combination of layout 1 and layout 3 (bending and shear zone).

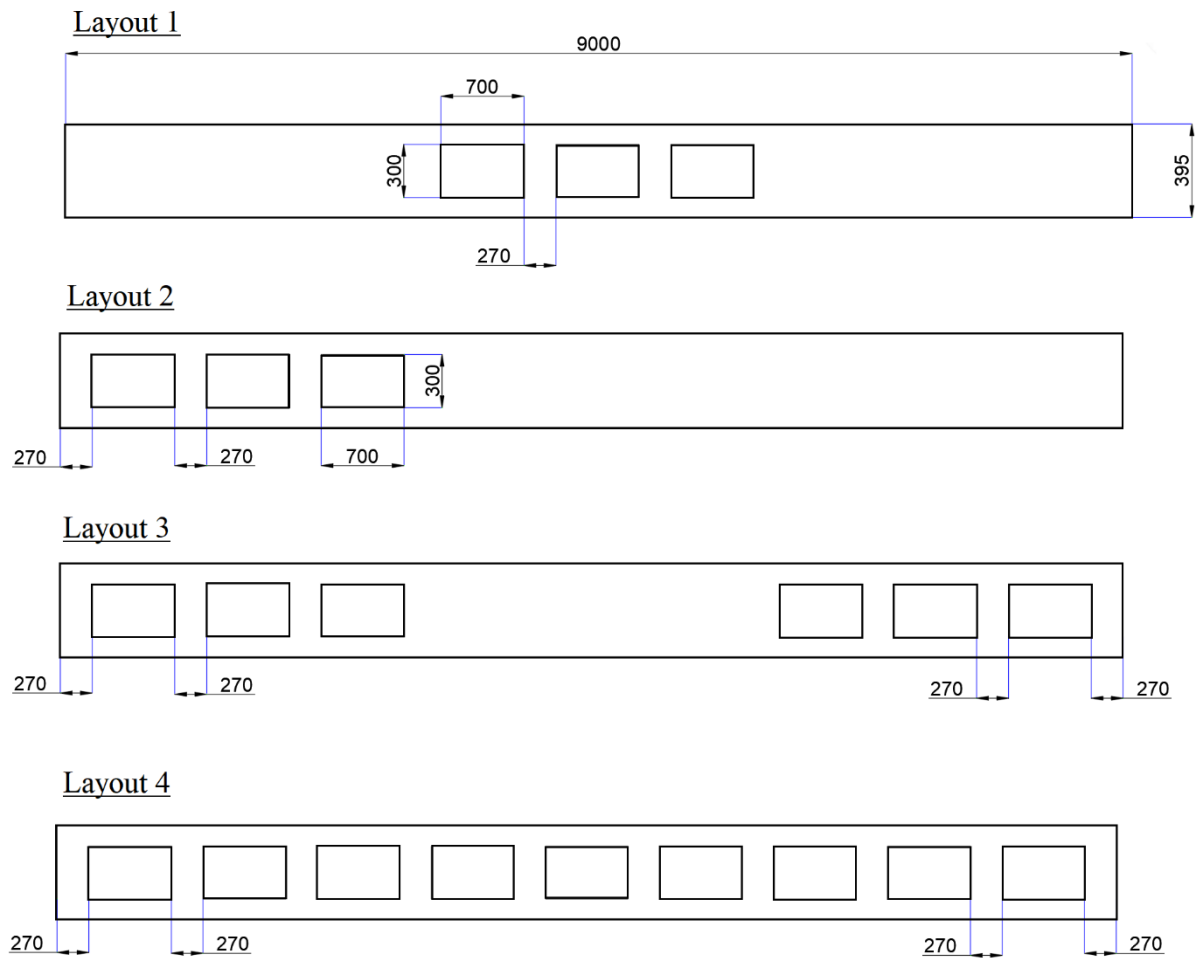


Fig. 9. Schematic of opening layout (all dimensions are in mm)

1
2
3
4
5
6
7
8
9
10
11
12
13
14
15
16
17

It is noteworthy that the load levels mentioned above result in different load ratios for each beam in the parametric study as the member capacity is related to the opening arrangement, steel grade, etc. The parametric study is divided into twelve different groups for ease of analysis. Each group comprises 3 simulations, all of which have the same opening layout and steel grade but a different applied load level (i.e. LL1, LL2 or LL3). Accordingly, groups 1, 5 and 9 correspond to beams with opening layout 1 and steel strength of 275, 450 and 550 N/mm², respectively. Similarly, groups 2, 6 and 10 investigate opening layout 2 whilst groups 3, 7 and 11 study layout 3 and groups 4, 8 and 12 contain beams with opening layout 4. All other material and geometric properties of the beam and surrounding structure are identical to that described earlier in the model validation and the Mokrsko AS4 test.

1 **Table 1.** Composite frames investigated in the parametric study

Group No.	Beam	Opening Layout	Steel Grade	LL	Group No.	Beam	Opening Layout	Steel Grade	LL
Group 1	Beam-1	Layout 1	275	LL1	Group 7	Beam-19	Layout 3	450	LL1
	Beam-2	Layout 1	275	LL2		Beam-20	Layout 3	450	LL2
	Beam-3	Layout 1	275	LL3		Beam-21	Layout 3	450	LL3
Group 2	Beam-4	Layout 2	275	LL1	Group 8	Beam-22	Layout 4	450	LL1
	Beam-5	Layout 2	275	LL2		Beam-23	Layout 4	450	LL2
	Beam-6	Layout 2	275	LL3		Beam-24	Layout 4	450	LL3
Group 3	Beam-7	Layout 3	275	LL1	Group 9	Beam-25	Layout 1	550	LL1
	Beam-8	Layout 3	275	LL2		Beam-26	Layout 1	550	LL2
	Beam-9	Layout 3	275	LL3		Beam-27	Layout 1	550	LL3
Group 4	Beam-10	Layout 4	275	LL1	Group 10	Beam-28	Layout 2	550	LL1
	Beam-11	Layout 4	275	LL2		Beam-29	Layout 2	550	LL2
	Beam-12	Layout 4	275	LL3		Beam-30	Layout 2	550	LL3
Group 5	Beam-13	Layout 1	450	LL1	Group 11	Beam-31	Layout 3	550	LL1
	Beam-14	Layout 1	450	LL2		Beam-32	Layout 3	550	LL2
	Beam-15	Layout 1	450	LL3		Beam-33	Layout 3	550	LL3
Group 6	Beam-16	Layout 2	450	LL1	Group 12	Beam-34	Layout 4	550	LL1
	Beam-17	Layout 2	450	LL2		Beam-35	Layout 4	550	LL2
	Beam-18	Layout 2	450	LL3		Beam-36	Layout 4	550	LL3

2 All of these analyses are conducted in two stages whereby the mechanical load is first applied
3 to the whole structure in both the OpenSEES and ABAQUS models and this is then followed
4 by the application of the thermal load in the detailed ABAQUS model of the perforated beam.
5 The same fire model (i.e. time-temperature relationship) as used in the model validation
6 previously described, is applied in all cases. Accordingly, the temperatures obtained from the
7 AS4 beam test are applied to all the groups as shown in the Fig. 3.

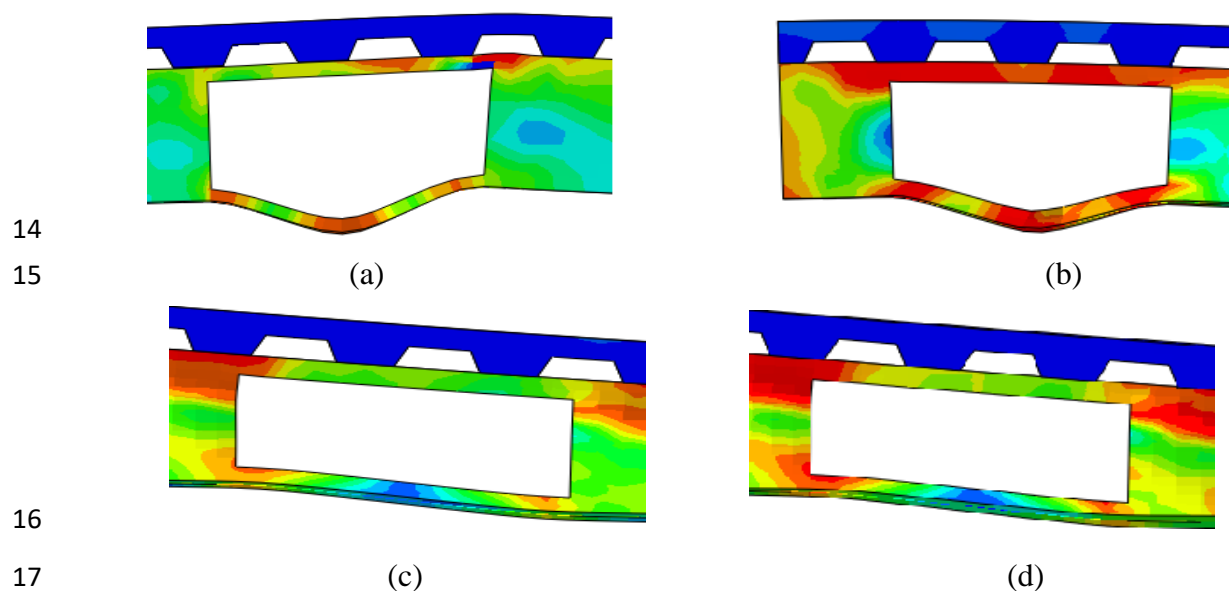
8 **RESULTS AND DISCUSSION**

9 In this section, the results of the parametric study using virtual hybrid simulation are presented
10 and discussed. Particular attention is given to analysing the fire resistance, vertical
11 displacement, axial restraint, local buckling and deflected shape in order to understand the
12 behaviour and assess the influence of the most critical parameters.

13 **Transition Time and Temperature**

14 The transition time refers to the point in the response at which the axial force in the beam
15 changes from compression to tension, as observed in Fig. 8. For a typical restrained perforated
16 beam in bending, as load is applied at ambient temperature, the top tee-section and slab

1 experience compression forces whereas the lower part of the beam goes into tension. With the
2 addition of fire loading, initially the restraint against thermal expansion results in an increase
3 in the compressive forces in the top of the beam and a reduction of the tensile forces in the
4 lower portion. Then, as the deflection increases and due to the thermal gradient across the depth
5 of the section, compressive arching occurs and the whole cross-section is in compression. Local
6 failure may occur either if the bottom tee-section buckles or yields under this compressive
7 stress or through the formation of a Vierendeel mechanism, depending on the position of the
8 opening; both of these local mechanisms are presented in Fig. 10 for the 4 opening layouts. As
9 deflections increase further, the compressive forces begin to reduce in the section. Web-post
10 buckling and web buckling due to lateral movement of the lower flange may develop and the
11 axial force in the beam changes from compression to tension. The time at which this occurs is
12 known as the transition time and the temperature at which this change takes place is the
13 transition temperature.

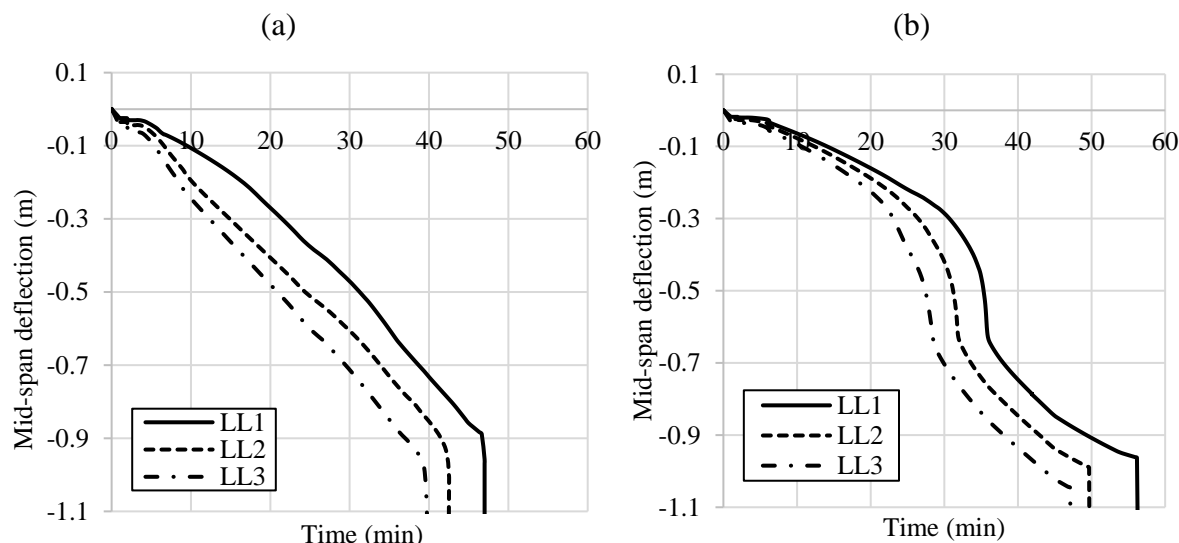
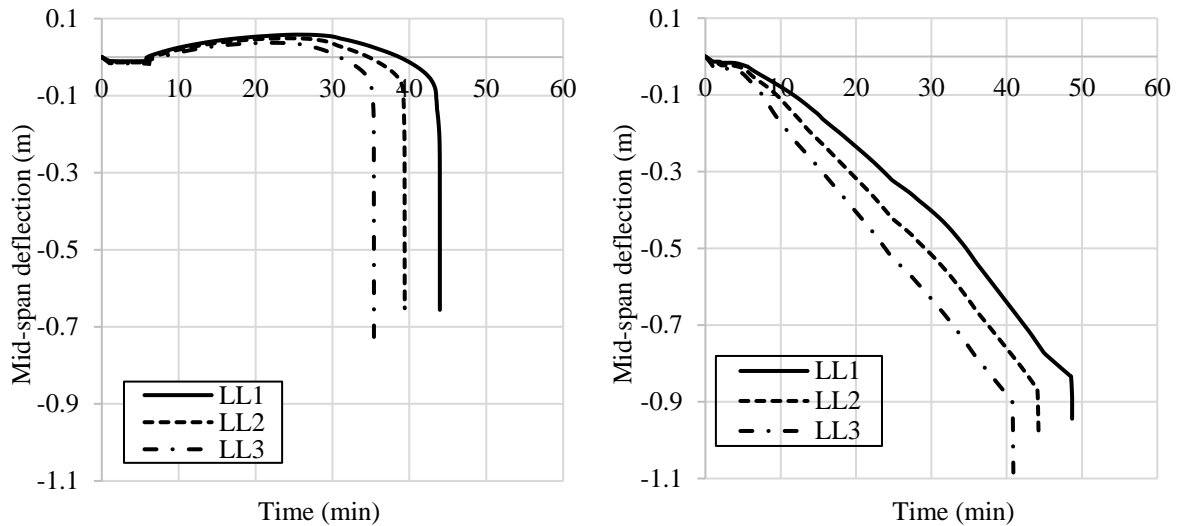


20 Fig. 10. Local failure modes for beams made with steel S275 for opening layout (a) 1, (b) 2,
21 (c) 3 and (d) 4

22 *Load Level*

23 Fig.11 presents the mid-span deflection versus time responses for beams in Group 1 to Group
24 4 with different opening layouts and load levels whilst Fig. 12 illustrates the axial force
25 response against time for the same beams. With reference firstly to Fig. 11, it is observed that
26 in general the overall behaviour remains unchanged irrespective of the load level. The response
27 is quite different depending on the opening layout and each of the figures in Fig. 11(a) to (d)
28 presents differently shaped curves (this will be discussed further in Section Opening Layout).
29 As expected, an increase in the load level results in greater mid-span deflections for a given
time, as well as an earlier transition time and ultimate failure. It is observed that for layout 2, 3
and 4, presented in Fig. 11(b) to (d), respectively, the beam deflects in a downward direction

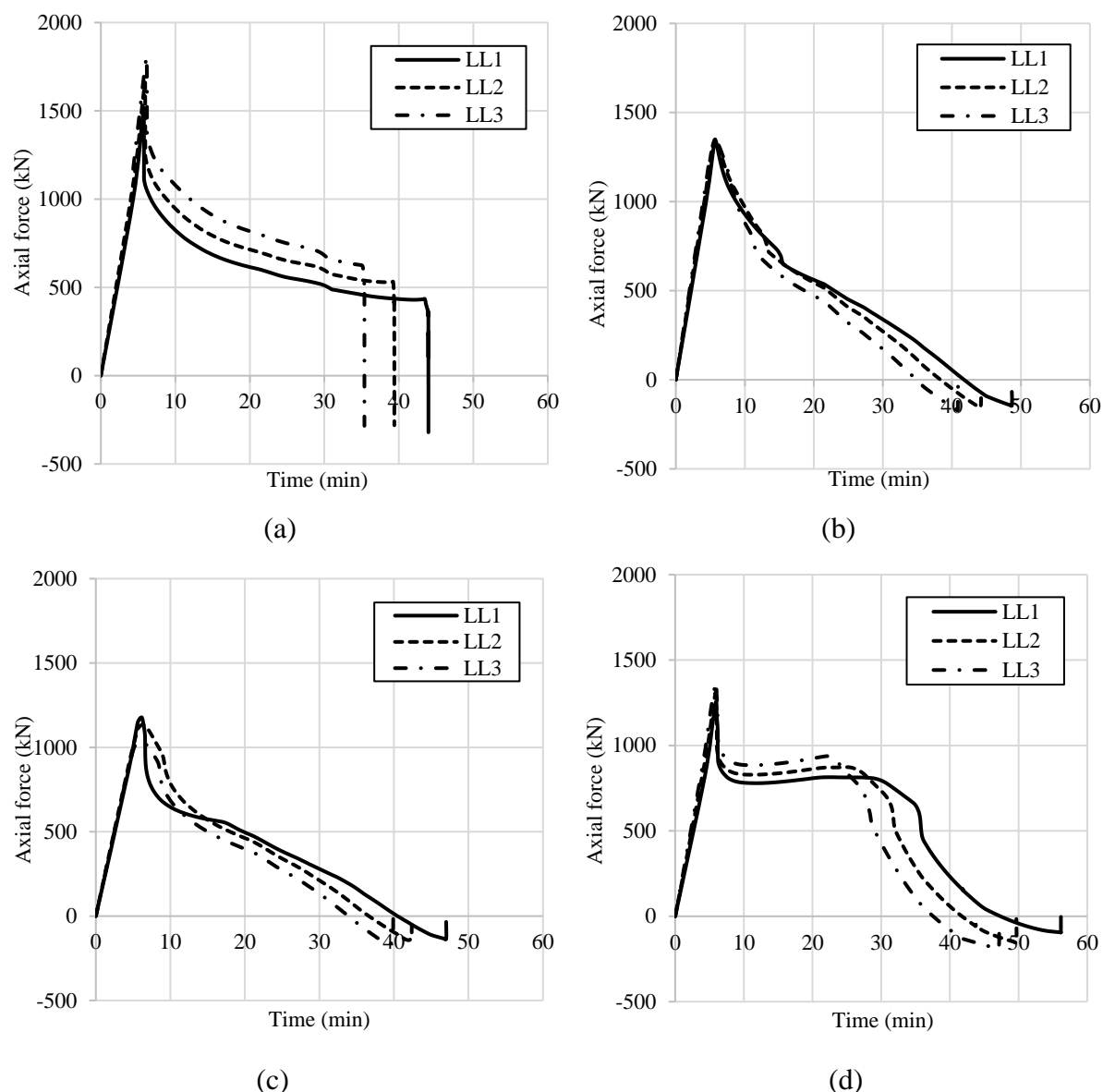
1 from the beginning of the analysis. However, for layout 1 (Fig. 11(a)), the beam initially
2 deflects upwards for all load levels. As shown previously in Fig. 3, the temperature in the
3 bottom flange increases much more rapidly compared with the temperature of the web, top
4 flange and the slab.



9 Fig. 11. Time-deflection behaviour for beams made with steel strength S275 and opening
10 layout (a) 1, (b) 2, (c) 3 and (d) 4.

11 As a result, initially, the compressive force in the bottom tee due to the restrained thermal
12 expansion is greater than that in the top tee and slab causing a hogging moment to develop with
13 corresponding upward deflections. For layout 1, the opening is at the centre of the beam and
14 therefore the section is weaker at this location and the beam tends to deflect in an upward
15 direction as it initially behaves somewhat like two separate cantilever beams under hogging
16 moments. Arching action also develops in the beam and the applied load induces more

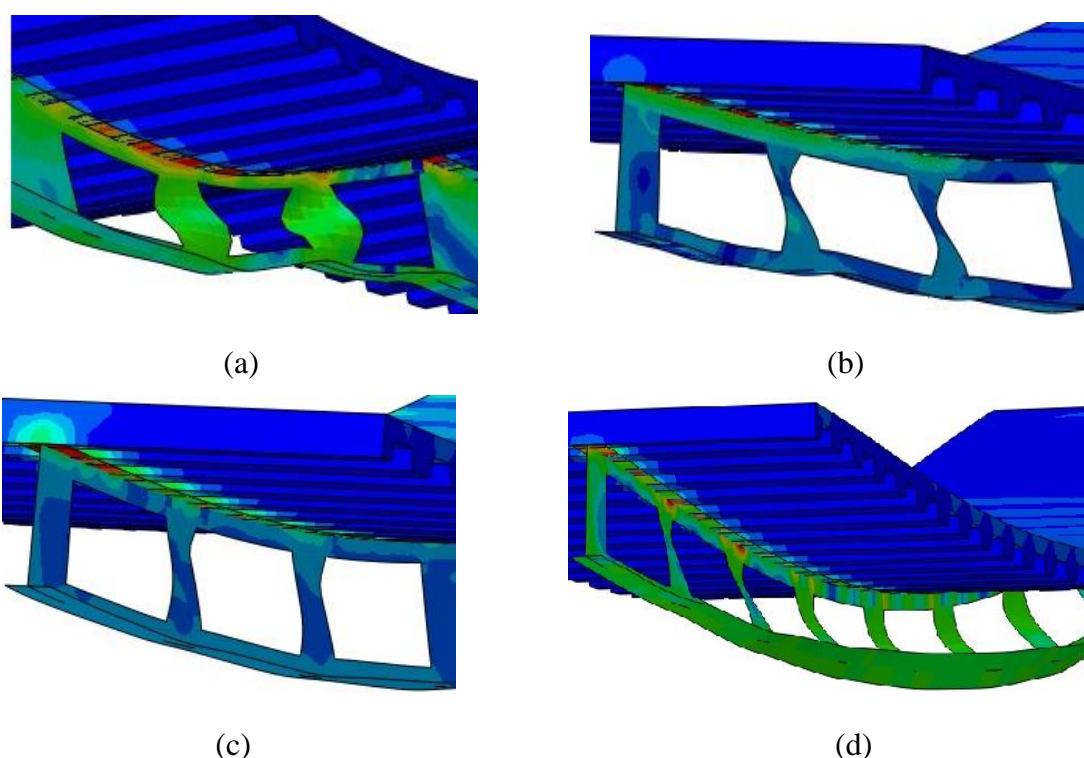
1 compressive forces in the section. Owing to this, the bottom tee section yields and the web-
2 post begins to buckle causing the beam to eventually deflect in a downward direction.



3
4
5
6
7
8 Fig. 12. Development of axial force for beams made with S275 at different load level and
9 opening layout (a) 1, (b) 2, (c) 3 and (d) 4.

10 With reference to Fig. 12, similar behaviour is observed for all perforated composite beams
11 with the same opening layout, regardless of steel strength and load level applied. In general, it
12 is noteworthy that the peak axial force value in the beams is much greater for layout 1 than for
13 the other opening arrangements. These beams have openings in the bending zone, which results
14 in the development of arching action and a greater axial force. For layouts 2 and 3 which have
15 openings in the shear zone only, arching action does not develop and therefore the levels of
16 axial forces in the beam are lower. For beams with opening layout 4, some arching action does

1 develop but because the relative stiffness of the section is similar along the whole length of the
2 beam, only a small portion of the hogging moment is transferred to the mid-section, which
3 leads to the development of partial arching action. The local failure modes including web-post
4 buckling, buckling of the bottom flange and the lateral displacement of the web is presented in
5 Fig. 13 for each of the layouts. Buckling of the web-post and lower flange is observed for all
6 the opening layouts due to the narrow width of the web-post. On the other hand, the top flange
7 remains straight and buckling is prevented by the slab. Of the four layouts studied, only layout
8 4 results in lateral displacement of the web which is attributed to the reduced stiffness of the
9 web in this arrangement owing to the presence of openings along the whole span.

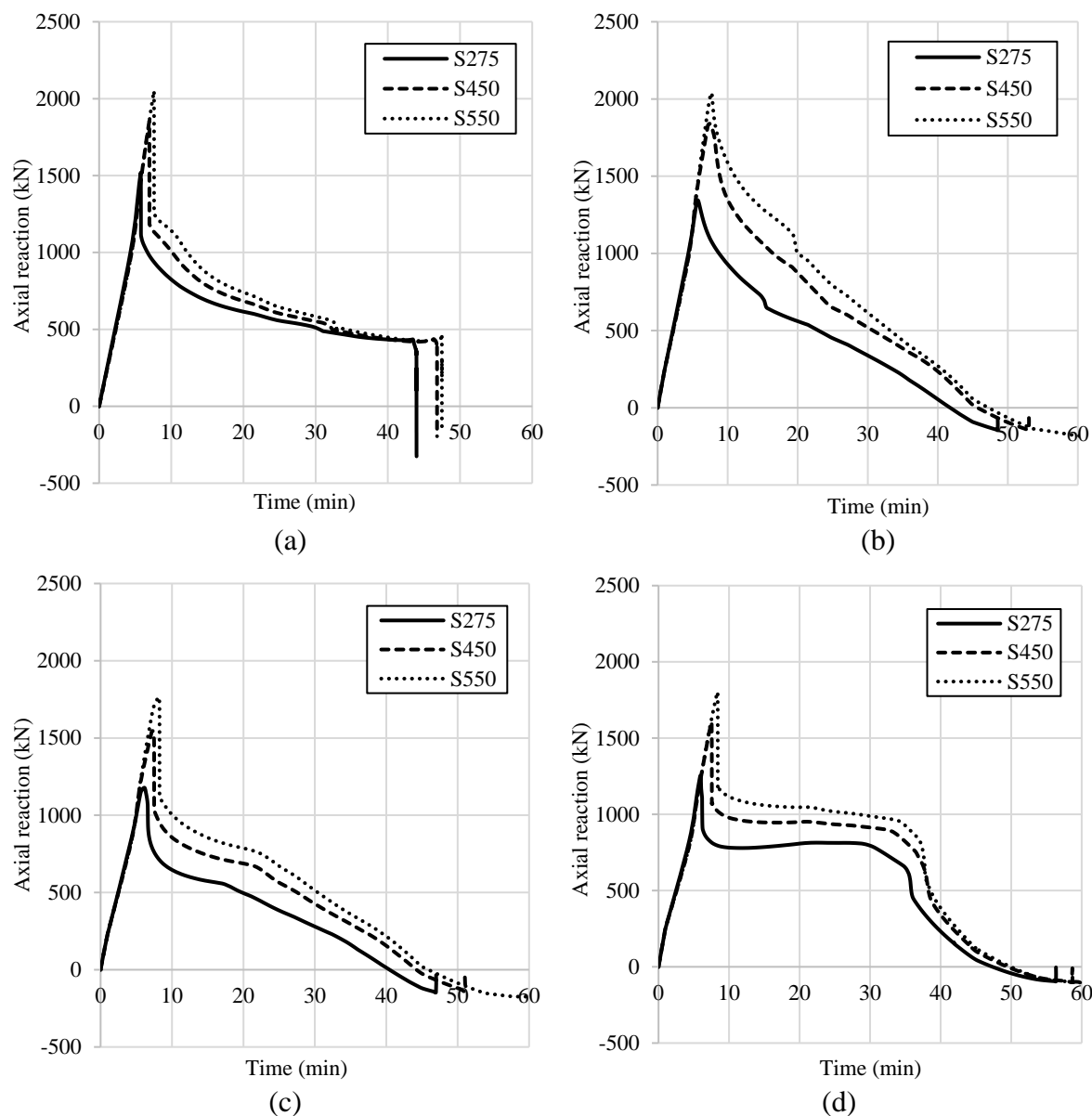


14 Fig. 13. Web-post buckling and lateral torsional displacement for beams made with S275 and
15 opening layout (a) 1, (b) 2, (c) 3 and (d) 4.

16 *Steel Grade*

17 In this section, the influence of different grades of steel on the overall behaviour is assessed.
18 As given in Table 1, three different grades are included in the study, with yield strengths of
19 275, 450 and 550 N/mm², respectively. Fig. 14 presents the development of axial force in the
20 beam for each steel type, in the 4 different layout arrangements. It is shown that greater axial
21 force develops in the beams made from relatively stronger steel, as expected. Moreover, the
22 beams made from S275 steel start behaving as a tensile catenary earlier than the beams with
23 higher steel strength. The magnitude of the axial reaction provides an indication of the stiffness
24 and strength of the beam relative to the surrounding structure. An increase in steel strength has
25 a positive effect on the web-post buckling and lateral torsional buckling behaviour and the out-

1 of-plane displacements of the web-post are reduced. It is noteworthy that although there is a
2 difference in the axial force between beams made from S450 and S550, the transition time is
3 almost identical. Therefore, any further increase in the steel strength may not give any
4 improvement in terms of fire resistance for perforated beams.



5
6
7
8
9 Fig. 14. Development of axial force for beams made with different strength steels and
10 opening layout (a) 1, (b) 2, (c) 3 and (d) 4.

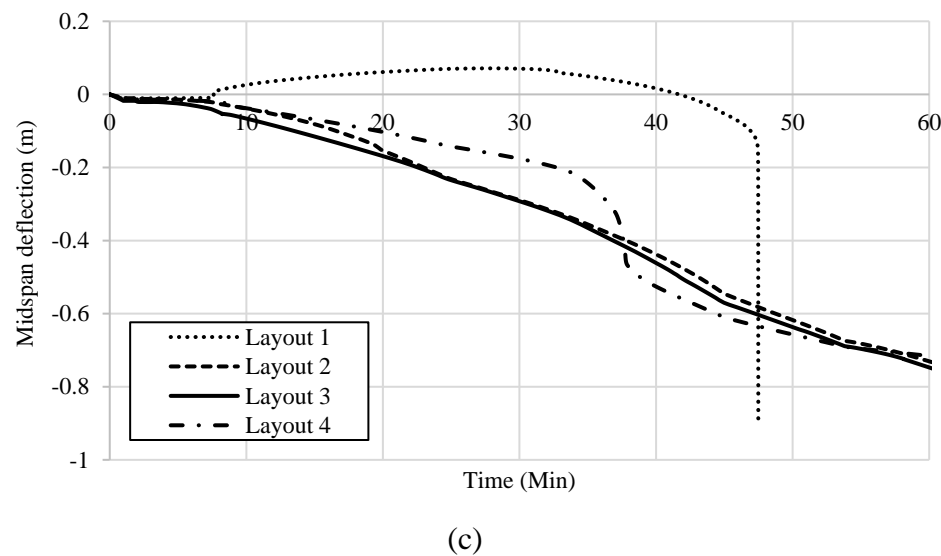
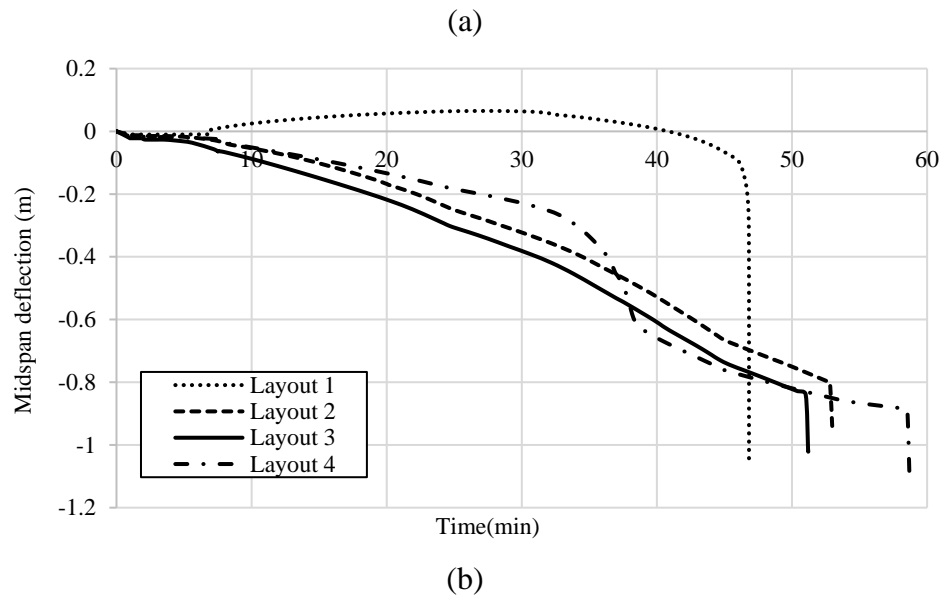
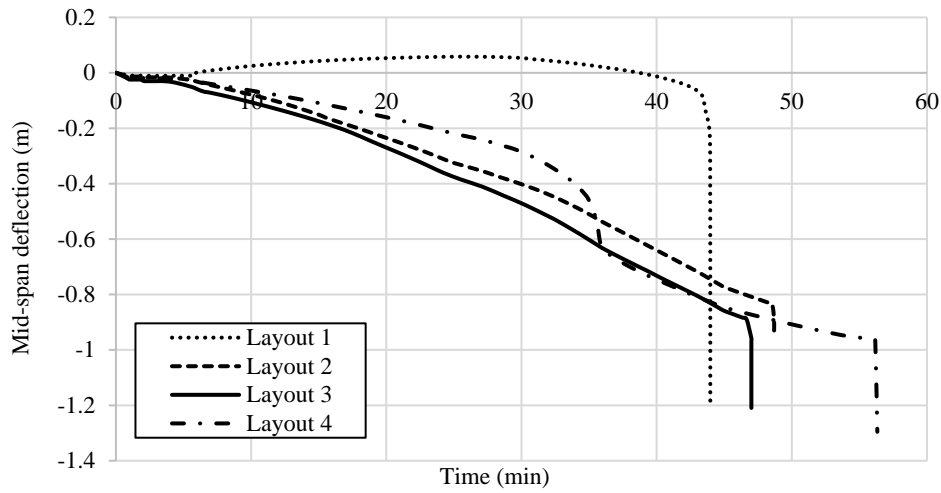
11 *Opening Layout*

12 It has already been presented that the arrangement of openings in the perforated beam can be
13 highly influential to the overall performance in fire and this will be discussed further in this
14 section. Towards this end, Figs. 15 and 16 presents the development of both vertical mid-span
15 deflection and axial force, with time, for perforated composite beams made from S275, S450

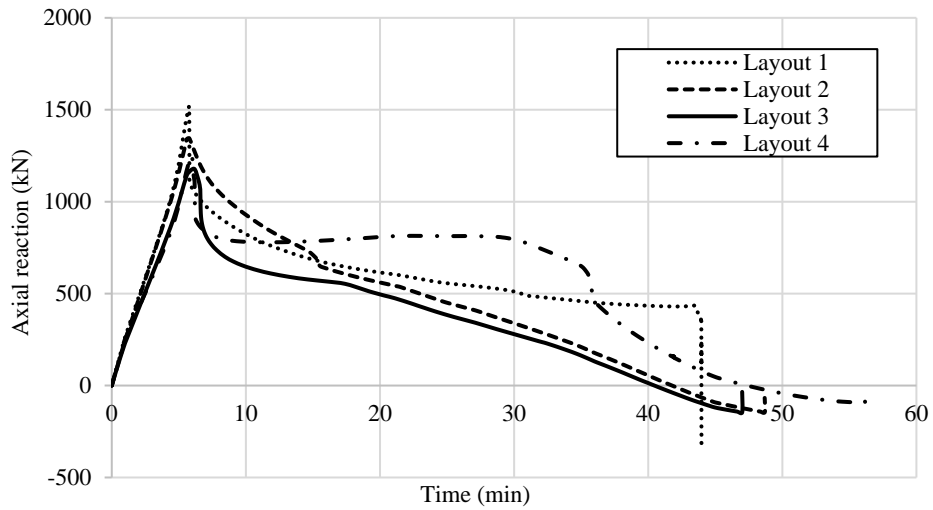
1 and S550 steel, respectively. From these figures, it is clear that the presence of openings is very
2 influential to the behaviour and a number of observations are made, as follows:

- 3 • All beams with layout 1 (which has an opening in the bending zone only) experience an
4 initial upward deflection initially before the beam changes direction and starts moving
5 downwards. This then results in the development of less arching action and a later transition
6 time as well as a lower ultimate displacement, compared with beams that do not have
7 openings in the bending area.
- 8 • The area of the openings in layout 1 is identical to that in layout 2 as shown in Fig. 9, but
9 the mid-span deflections are much lower for the former arrangement, irrespective of load
10 ratio or steel strength which is illustrated in Fig. 15. This is because the beam with openings
11 in layout 1 experiences both bending and axial compression and the behaviour is influenced
12 by buckling of the bottom tee as well as web-post buckling. On the other hand, layout 2 only
13 has openings in the shear zone and develops relatively less axial compression in the absence
14 of arching action. The development of an arching action in the beams with layout 1 reduces
15 the midspan deflection considerably.
- 16 • For beams that have openings in the bending zone (i.e. layout 1 and 4), the behaviour is
17 governed by the buckling resistance of the bottom tee at the openings. On the other hand,
18 for beams with openings in the shear zone, these must be able to resist Vierendeel bending
19 in addition to bending and axial compression. In the Vierendeel mechanism, transverse shear
20 is transferred across the opening leading to the formation of plastic hinges at the corners of
21 the opening. In the later stages of a fire (i.e. after 15 minutes), the reduction in compression
22 forces in layout 1 and 4 is gradual and the transition time is relatively high compared to
23 Layout 2 and 3, as shown in Fig.16.
- 24 • The degree of web-post buckling in layout 1 and lateral displacement of the web for beams
25 with layout 4 is greater than the beams with opening layout 2 or 3 due to the presence of the
26 openings in the bending zone.
- 27 • Transition time is an important concept in structural fire engineering as it indicates the fire
28 resistance of the beam in a given fire scenario. For the cases considered herein, at the
29 transition time, the beam is no longer resisting the applied loads through bending action but
30 by acting as a tensile catenary. The transition time is greatest for opening layout 4, followed
31 by layout 1, 2 and 3, respectively. It is clear that beams with openings in layout 1 fail
32 suddenly as shown in Fig. 15 and Fig. 16, whereas all other cases considered in this study
33 continue to carry load through the development of catenary action. For layout 4, the presence
34 of openings along the whole length of the beam helps in distributing the load uniformly
35 across the span, which delays failure, compared with the other layouts. The development of
36 arching action reduces the mid-span deflections and keeps the beam in compression for
37 longer, which delays the transition time and therefore improves the fire resistance. It is

1 noteworthy that layouts 2 and 3 behave very similarly with similar transitions times, despite
2 layout 3 having an additional set of openings.

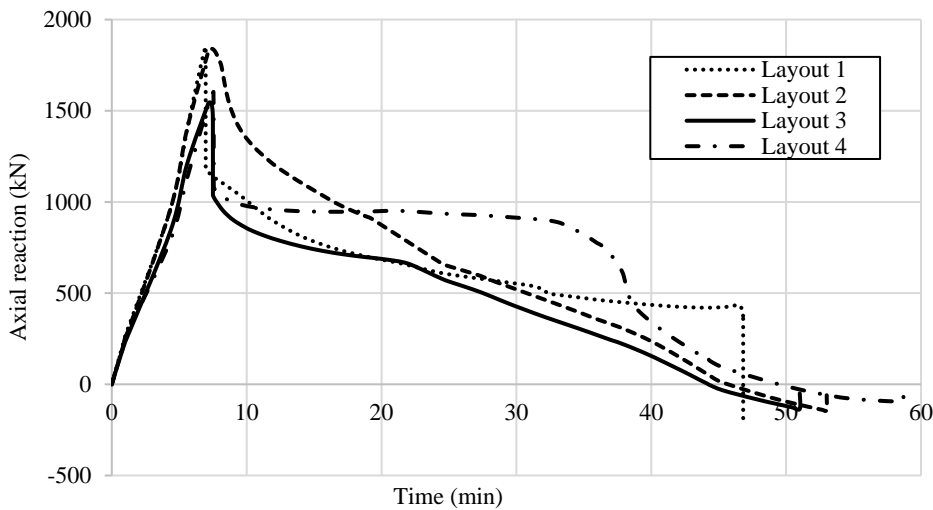


9 Fig. 15. Midspan deflection variation for all layouts, a) Steel grade 275 N/mm² b) Steel
10 grade 450 N/mm² c) Steel grade 550 N/mm²



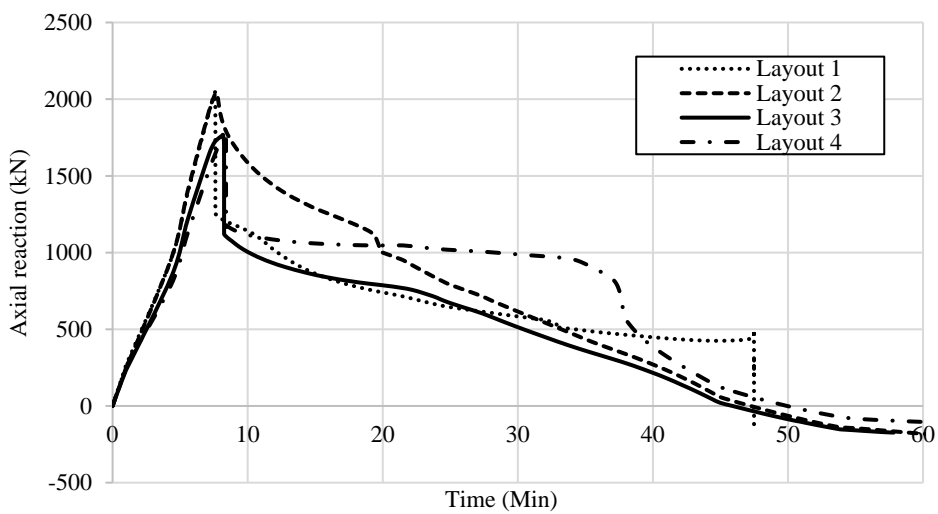
1
2

(a)



3
4

(b)



5
6

(c)

7 Fig. 16. Axial reaction variation for all layouts, a) Steel grade 275 N/mm² b) Steel grade 450
8 N/mm² c) Steel grade 550 N/mm²

1 **COMPARISON WITH DESIGN CODES**

2 In this section, the fire resistance of the 36 perforated composite beams presented in Table 1 is
3 compared with the design values obtained using the SCI P355 design guide (Lawson and Hicks
4 1998) by applying reduction factors from Eurocode 4 (EN-1994-1-2 2005), which covers the
5 design of composite beams with large web openings. As P355 only covers the ambient
6 temperature response, the design equations are modified by applying the elevated temperature
7 reduction factors given in Eurocode 4. The critical temperature is defined as the point at which
8 the beam fails and the failure modes considered are bending, shear, Vierendeel bending and
9 web-post buckling. Once the critical temperature is established, the fire resistance can be
10 estimated.

11 Table 2 presents the results including the fire resistance predicted by the finite element
12 simulation ($R_{fi,FEM}$), SCI P355 ($R_{fi,P355}$) and also the ratio of these two values. It is shown
13 that in almost all cases, the finite element analysis predicts that the beams will last for a longer
14 period of time before failure occurs, compared with the design code. It is important to note that
15 the design equations do not account for axial restraint and assume simply-supported boundary
16 conditions. It has been shown in previous studies that restrained beams offer greater fire
17 resistance compared with unrestrained beams (British Steel Plc 1999; Izzuddin and Moore
18 2002). With reference to Table 2, it can be seen that beams with opening layout 2, 3 or 4 have
19 identical fire resistance according to the design equations because the behaviour is governed
20 by the Vierendeel mechanism and buckling of the web-post in the shear zone. Therefore, these
21 equations do not account for the effect of multiple openings at various locations. On the other
22 hand, the finite element analysis considers all of the influential aspects such as opening shape
23 and location as well as the arching effect due to axial restraint. For opening layout 1, the fire
24 resistance estimated using finite element simulation is lower than the fire resistance computed
25 using design equations. This behaviour is due to the sudden failure of these beams at the onset
26 of the axial force transition from compression to tension. For most of the cases investigated in
27 this study, a close agreement is achieved between the design calculations and the simulations
28 and the slight differences are due to the above-mentioned factors. However for design purposes,
29 it is important to note that the analytical equations provide a conservative estimate of fire
30 resistance.

31

32

33

34

35

36

1 **Table 2.** Finite element analysis results and SCI-P355/EC-4 fire resistance

Group	Beam	$R_{fi,FEM}$ (min)	$R_{fi,P355}$ (min)	$R_{fi,FEM} / R_{fi,P355}$
Group 1	Beam-1	43	43	1
	Beam-2	39	41	0.95
	Beam-3	35	37	0.95
Group 2	Beam-4	48	43	1.12
	Beam-5	44	39	1.13
	Beam-6	41	33	1.24
Group 3	Beam-7	47	43	1.09
	Beam-8	42	39	1.08
	Beam-9	39	33	1.18
Group 4	Beam-10	56	43	1.3
	Beam-11	49	39	1.26
	Beam-12	47	33	1.42
Group 5	Beam-13	47	50	0.94
	Beam-14	43	47	0.91
	Beam-15	39	44	0.89
Group 6	Beam-16	52	50	1.04
	Beam-17	49	43	1.14
	Beam-18	46	39	1.18
Group 7	Beam-19	51	50	1.02
	Beam-20	47	43	1.09
	Beam-21	45	39	1.15
Group 8	Beam-22	58	50	1.16
	Beam-23	52	43	1.21
	Beam-24	48	39	1.23
Group 9	Beam-25	50	60	0.83
	Beam-26	46	50	0.92
	Beam-27	43	46	0.93
Group 10	Beam-28	60	60	1
	Beam-29	60	46	1.3
	Beam-30	56	42	1.33
Group 11	Beam-31	60	60	1
	Beam-32	55	46	1.2
	Beam-33	52	42	1.24
Group 12	Beam-34	60	60	1
	Beam-35	60	46	1.3
	Beam-36	57	42	1.36

1 CONCLUSIONS

2 This paper has presented the framework for performing a hybrid simulation type approach for
3 the analysis of restrained perforated beams subjected to fire, in a real building. Firstly, a
4 detailed description of the novel virtual hybrid simulation method was presented. This includes
5 the slave assembly, in ABAQUS, and the master assembly, implemented using the open-source
6 software OpenSEES. This virtual hybrid simulation approach offers both accuracy and
7 excellent computational efficiency, particularly for complex problems such as modelling a
8 whole building which is subjected to fire. Hybrid simulation, which includes physical testing,
9 has been extensively applied to seismic engineering applications. However, in order to develop
10 a framework for examining other extreme conditions such as fire, it is convenient to replace
11 the physical testing element with a detailed numerical assembly, as is developed herein.

12 The virtual hybrid simulation approach is validated for perforated beams subjected to fire using
13 available test data. Thereafter, the model is employed to conduct a parametric study. The key
14 variables included in the study are the opening position, steel strength and load level. During
15 the analysis of the results, it is noted that for axially restrained perforated composite beams,
16 there are a number of distinct stages during the response. Initially, at ambient temperature, the
17 section is in pure bending. Then, as the temperature increases, the whole section starts
18 experiencing axial compression owing to the restraint provided. As soon as initial yielding
19 occurs either by buckling of the bottom tee and web-post or by the Vierendeel mechanism,
20 these compression forces reduce. Beams with openings in the bending zone experience a more
21 rapid unloading compared with beams that have openings in the shear zone only. Thereafter,
22 with increasing deflection, the axial force in the section transitions from compression to tension
23 as the beam behaves as a tensile catenary. It is noted that compressive arching action develops
24 for all beams that have openings in the bending zone which delays the transition time of the
25 beam giving greater fire resistance.

26 The effect of load level on the fire behaviour of perforated beams has also been studied and it
27 is found that an increase in the load applied to the beam results in a relative reduction in the
28 transition time i.e., a reduction in the fire resistance of the beam. The overall behaviour remains
29 the same with a change in the load level and steel strength. As expected, beams made using a
30 higher strength steel grade demonstrate greater capacity to develop axial forces. Interestingly,
31 beams which have openings throughout their length are shown to offer the greatest fire
32 resistance of those examined in this study. This is due to the fact that the stresses and loads are
33 more evenly distributed across the length and the development of arching action provides a
34 significant mechanism for resisting the applied loads, supplementing the bending resistance.
35 On the other hand, beams which have openings in the bending zone only are shown to offer the
36 lowest fire resistance.

1 In terms of design, the current design equations which are available for the ambient temperature
2 response have been modified to include the effects of elevated temperature. It is shown that
3 this approach provides a good estimation of the fire resistance for most cases, apart from layout
4 1 of the studied arrangements. In all other cases, the fire resistance predicted by the virtual
5 hybrid simulation is greater compared with the fire resistance calculated using design
6 equations. This is mainly because the effects of axial and rotational restraint are accounted for
7 in the model. On the other hand, for design purposes, ignoring the effect of the support
8 restraints is shown to provide a conservative estimate of the fire resistance for the range of
9 parameters included in this study.

11 REFERENCES

- 12 ABAQUS. (2010). "ABAQUS Documentation, Dassault Systèmes, U.S.A." Dassault
13 Systèmes.
- 14 Abu, A., Block, F., Butterworth, N., and Burgess, I. (2009). "Structural fire engineering
15 assessments of the Fracof and Moksko fire tests: An Engineering prediction." *Application
16 of Structural Fire Engineering*, Prague, Czech Republic.
- 17 British Steel Plc. (1999). *The behaviour of multi-storey steel framed buildings in fire*. Swinden
18 Technology centre, Rotherham.
- 19 Dwaikat, M. M. S., and Kodur, V. K. R. (2011). "A performance based methodology for fire
20 design of restrained steel beams." *Journal of Constructional Steel Research*, 67, 510–524.
- 21 Ellobody, E., and Young, B. (2015). "Nonlinear analysis of composite castellated beams with
22 profiled steel sheeting exposed to different fire conditions." *Journal of Constructional
23 Steel Research*, 113, 247–260.
- 24 EN-1994-1-2. (2005). "Eurocode 4: Design of composite steel and concrete structures - Part 1-
25 2 General rules - Structural fire design." *European Committee for Standardization*,
26 Brussels.
- 27 EN 1992-1-2. (2004). "Eurocode 2: Design of concrete structures - Part 1-2: General rules -
28 Structural fire design." *European Committee for Standardization*, Brussels.
- 29 EN 1993-1-2. (2005). "Eurocode 3: Design of steel structures - Part 1-2: General rules -
30 Structural fire design." *European Committee for Standardization*, Brussels.
- 31 Franssen, J. M., and Gernay, T. (2017). "Modeling structures in fire with SAFIR®: Theoretical
32 background and capabilities." *Journal of Structural Fire Engineering*, 8(3), 300–323.
- 33 Izzuddin, B. A., and Moore, D. B. (2002). "Lessons from a full-scale fire test." *Proceedings of
34 the ICE - Structures and Buildings*, 152(4), 319–329.
- 35 Jiang, J., Jiang, L., Kotsovinos, P., Zhang, J., and Usmani, A. (2015). "OpenSEES Software
36 Architecture for the Analysis of Structures in Fire." *Journal of Computing in Civil
37 Engineering*, 29(1), 04014030.
- 38 Jiang, L., and Usmani, A. (2018a). "Towards scenario fires – modelling structural response to
39 fire using an integrated computational tool." *Advances in Structural Engineering*, 21(13),
40 2056–2067.
- 41 Jiang, L., and Usmani, A. (2018b). "Computational performance of beam-column elements in

- 1 modelling structural members subjected to localised fire.” *Engineering Structures*,
2 Elsevier, 156(June 2017), 490–502.
- 3 Khan, M. A., Jiang, L., Cashell, K. A., and Usmani, A. (2018). “Analysis of restrained
4 composite beams exposed to fire using a hybrid simulation approach.” *Engineering*
5 *Structures*, Elsevier, 172(May), 956–966.
- 6 Kolozvari, K., Orakcal, K., and Wallace, J. W. (2018). “New OpenSEES models for simulating
7 nonlinear flexural and coupled shear-flexural behavior of RC walls and columns.”
8 *Computers and Structures*, 196, 246–262.
- 9 Kwon, O.-S., Nakata, N., Park, K., Elnashai, A., and Spencer, B. (2007). *User Manual and*
10 *Examples for UI-SIMCOR v2.6 (Multi-Site Substructure Pseudo-Dynamic Simulation*
11 *Coordinator) and NEES-SAM v2.0 (Static Analysis Module for NEESgrid).*
- 12 Lawson, R. M., and Hicks, S. J. (1998). “Design of beams with large web openings.” *Steel*
13 *Construction Institute*, Berkshire.
- 14 Li, G. Q., and Guo, S. X. (2008). “Experiment on restrained steel beams subjected to heating
15 and cooling.” *Journal of Constructional Steel Research*, 64, 268–274.
- 16 Liu, T. C. H., Fahad, M. K., and Davies, J. M. (2002). “Experimental investigation of behaviour
17 of axially restrained steel beams in fire.” *Journal of Constructional Steel Research*, 58,
18 1211–1230.
- 19 McKenna, F., Scott, M. H., and Fenves, G. L. (2009). “Nonlinear Finite-Element Analysis
20 Software Architecture Using Object Composition.” *Journal of Computing in Civil*
21 *Engineering*, 24(1), 95–107.
- 22 McKenna, F. T. (1997). “Object-oriented finite element programming: Frameworks for
23 analysis, algorithms and parallel computing.” *ProQuest Dissertations and Theses*.
- 24 Mostafaei, H. (2013). “Hybrid fire testing for assessing performance of structures in fire -
25 Methodology.” *Fire Safety Journal*, Elsevier, 58, 170–179.
- 26 Nadjai, A., Bailey, C. G., Vassart, O., Han, S., Zhao, B., Hawes, M., Franssen, J. M., and
27 Simms, I. (2011). “Full-scale fire test on a composite floor slab incorporating long span
28 cellular steel beams.” *Structural Engineer*, 89(21), 18–25.
- 29 Nadjai, A., Han, S., Ali, F., Alam, N., and Allam, A. (2017). “Fire resistance of axial restraint
30 composite floor steel cellular beams.” *Journal of Constructional Steel Research*, 136,
31 229–237.
- 32 Nadjai, A., Petrou, K., Han, S., and Ali, F. (2016). “Performance of unprotected and protected
33 cellular beams in fire conditions.” *Construction and Building Materials*, Elsevier Ltd,
34 105, 579–588.
- 35 Nadjai, A., Vassart, O., Ali, F., Talamona, D., Allam, A., and Hawes, M. (2007). “Performance
36 of cellular composite floor beams at elevated temperatures.” *Fire Safety Journal*, 42(6–
37 7), 489–497.
- 38 Najafi, M., and Wang, Y. C. (2017a). “Axially restrained steel beams with web openings at
39 elevated temperatures, Part 1: Behaviour and numerical simulation results.” *Journal of*
40 *Constructional Steel Research*, 128, 745–761.
- 41 Najafi, M., and Wang, Y. C. (2017b). “Axially restrained steel beams with web openings at
42 elevated temperatures, Part 2: Development of an analytical method.” *Journal of*
43 *Constructional Steel Research*, 128, 687–705.

- 1 Sauca, A., Gernay, T., Robert, F., Tondini, N., and Franssen, J.-M. (2018). “Hybrid fire testing:
2 Discussion on stability and implementation of a new method in a virtual environment.”
3 *Journal of Structural Fire Engineering*, JSFE-01-2017-0017.
- 4 Schellenberg, A., Huang, Y., and Mahin, S. A. (2008). “Structural FE-software coupling
5 through the experimental software framework , openfresco.” *The 14th World Conference*
6 *on Earthquake Engineering*, 1–8.
- 7 Takahashi, Y., and Fenves, G. L. (2006). “Software framework for distributed experimental-
8 computational simulation of structural systems.” *Earthquake Engineering and Structural*
9 *Dynamics*, 35(3), 267–291.
- 10 Wald, F., Kallerová, P., Chlouba, P., and Sokol, Z. (2011). *Fire test on administrative building.*
11 *Steel and Aluminium Structures*, Mokrsko.
- 12 Wang, X., Kim, R. E., Kwon, O.-S., and Yeo, I. (2018). “Hybrid Simulation Method for a
13 Structure Subjected to Fire and Its Application to a Steel Frame.” *Journal of Structural*
14 *Engineering*, 144(8), 04018118.
- 15 Whyte, C. A., Mackie, K. R., and Stojadinovic, B. (2016). “Hybrid Simulation of
16 Thermomechanical Structural Response.” *Journal of Structural Engineering*, 142(2),
17 04015107.
- 18 Wong, V. B., Bruggess, I., and Plank, R. (2009). “Behaviour of composite cellular steel -
19 concrete beams at elevated temperatures.” *Steel Structures*, 9, 29–37.
- 20 Zhan, H., and Kwon, O. (2015). “Actuator controller interface program for pseudo-dynamic
21 hybrid simulation.” *Advances in Structural Engineering and Mechanics (ASEM15)*.
- 22 Zhu, M., McKenna, F., and Scott, M. H. (2018). “OpenSEESPy: Python library for the
23 OpenSEES finite element framework.” *SoftwareX*, Elsevier B.V., 7, 6–11.
- 24
- 25